

## PHYSICS

# Dipole moment background measurement and suppression for levitated charge sensors

Nadav Priel<sup>1\*</sup>, Alexander Fieguth<sup>1</sup>, Charles P. Blakemore<sup>1</sup>, Emmett Hough<sup>1</sup>, Akio Kawasaki<sup>1,2†</sup>, Denzal Martin<sup>1‡</sup>, Gautam Venugopalan<sup>1</sup>, Giorgio Gratta<sup>1,2</sup>

Optically levitated macroscopic objects are a powerful tool in the field of force sensing, owing to high sensitivity, absolute force calibration, environmental isolation, and the advanced degree of control over their dynamics that have been achieved. However, limitations arise from the spurious forces caused by electrical polarization effects that, even for nominally neutral objects, affect the force sensing because of the interaction of dipole moments with gradients of external electric fields. Here, we introduce a technique to measure, model, and eliminate dipole moment interactions, limiting the performance of sensors using levitated objects. This process leads to a noise-limited measurement with a sensitivity of  $3.3 \times 10^{-5} e$ . As a demonstration, this is applied to the search for unknown charges of a magnitude much below that of an electron or for exceedingly small unbalances between electron and proton charges.

## INTRODUCTION

Optical levitation of macroscopic objects in vacuum has recently drawn considerable attention due to numerous applications in the fields of sensing, quantum physics, and particle physics (1). The versatility of this technique stems from the ability to measure and control the translation, rotation, charge state, and dynamics of a macroscopic object with high precision (2–12), where the thermal and electrical isolation of the levitated object from the environment make the low-noise conditions possible.

Work with levitated dielectric microspheres (MSs) with masses in the range of 0.1 to 10 ng and force sensitivity of  $\approx 10^{-18} \text{ N}/\sqrt{\text{Hz}}$  can be applied to the investigation of phenomena beyond the Standard Model (BSM) of particle physics, including the search for a fifth force at short range (13–16), the breakdown of Coulomb's law as a probe for a dark photon (17), high-frequency gravitational wave detection (18, 19), and others (20–23). Each such endeavor is eventually expected to be limited by spurious electromagnetic interactions, ultimately limiting its sensitivity. Even for electrically neutral levitated objects, such backgrounds arise from the coupling between the higher-order electric multipole moments of the MS to the electromagnetic drive and sensing fields (24, 25), or to minute electric field gradients due to patch or contact potentials (14, 15, 26). In the broader context of experimental physics, systematic effects from residual interactions of nonuniform charge distributions have long plagued precision measurements (27–31).

In this work, we develop a model of those minute electromagnetic interactions with an optically trapped MS and demonstrate a technique capable of identifying and eliminating the unwanted contributions. This process enables noise-limited charge sensing at a level of  $3.3 \times 10^{-5} e$  for macroscopic objects.

An obvious application of a macroscopic charge sensor with understood dynamics is to probe the net neutrality of the sensor itself.

The resulting value can be interpreted two ways with respect to the Standard Model of particle physics. First, it can test the equality of magnitude of the proton and electron charges, complementing different techniques (32–34). Second, it can probe the existence of mini-charged particles (MCPs) (35, 36). Such particles, not included in Standard Model, could help answer central questions in physics, such as how and why charge is quantized (37, 38), and can also contribute to solve the dark matter puzzle (39–42).

In more general terms, the new understanding of the electromagnetic dynamics presented here significantly enhances the power of BSM searches with optical levitation technique by allowing discovery potential. In addition, this approach enables precision studies of the dielectric properties, e.g., polarizability, of levitated MSs.

## RESULTS

### Experimental setup

The centerpieces of the experiment described here are silica (43) MSs, with a diameter of  $(7.52 \pm 0.18) \mu\text{m}$  (44), trapped through optical forces exerted by a 1064-nm optical tweezer (45) arrangement in vacuum. A schematic of the experimental setup is shown in Fig. 1. The position of an MS in the horizontal ( $xy$ ) plane is obtained by measuring the deflection of the transmitted portion of the trapping laser beam on a quadrant photodiode, while the vertical ( $z$ ) position is obtained from the phase of the light retroreflected by the MS (44, 46). The optical trap is operated inside a vacuum chamber at  $\mathcal{O}(10^{-6} \text{ hPa})$ , and active feedback is used to cool the three translational degrees of freedom of the MS. With this setup, a force sensitivity of  $< 10^{-16} \text{ N}/\sqrt{\text{Hz}}$  has been achieved, which determines the ultimate sensitivity to any signal from the measurements presented here. The trap is closely surrounded by six identical electrodes shaped as truncated pyramids forming a cubic cavity. Each electrode is hollowed out and, on the trap end, terminates with an aperture providing optical and mechanical access to the center. Two distinct optical traps have been used for the measurements described here. The main difference between the traps is the separation between the faces of the electrodes and, hence, the size of the cubic region where the MS is trapped. The first setup, detailed in (46), has the electrodes of 8.6 mm apart and an aperture size of 5.3 mm, while the second, described in

Copyright © 2022  
The Authors, some  
rights reserved;  
exclusive licensee  
American Association  
for the Advancement  
of Science. No claim to  
original U.S. Government  
Works. Distributed  
under a Creative  
Commons Attribution  
NonCommercial  
License 4.0 (CC BY-NC).

<sup>1</sup>Department of Physics, Stanford University, Stanford, CA 94305, USA. <sup>2</sup>W.W. Hansen Experimental Physics Laboratory, Stanford University, Stanford, CA 94305, USA.

\*Corresponding author. Email: nadavp@stanford.edu

†Present address: National Metrology Institute of Japan (NMIJ), National Institute of Advanced Industrial Science and Technology (AIST), 1-1-1 Umezono, Tsukuba, Ibaraki 305-8563, Japan.

‡Present address: Los Alamos National Laboratory, Los Alamos, NM 87545, USA.

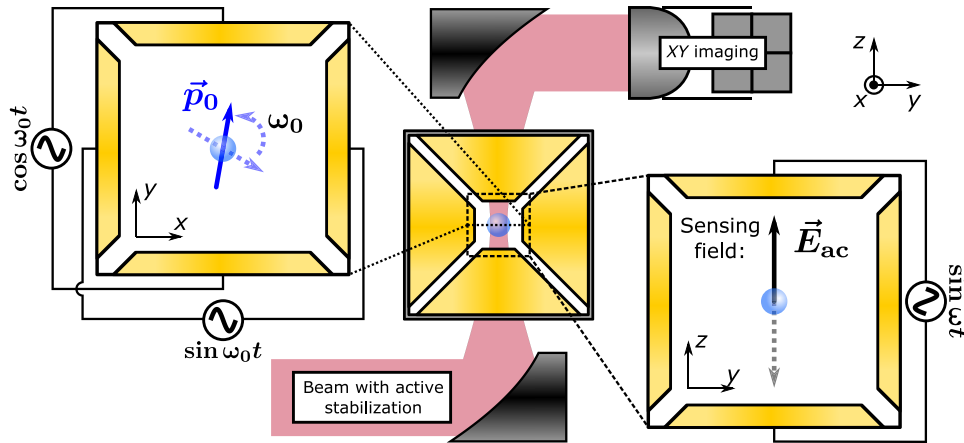


**Fig. 1. Schematic of the setup.** Schematic of the optical trap setup, with an MS at the center of the electrode cube structure. For clarity, the background and foreground electrodes have been omitted. A detail of the  $xy$  plane is shown on the left, indicating the driven rotation of the dipole moment at  $\omega_0 \sim 2\pi(100 \text{ kHz})$  using the four horizontal electrodes,  $x^+$  and  $y^+$ . A detail of the  $yz$  plane is shown to the right, indicating the sensing field applied along the  $z$  axis (vertical). This orientation of electric fields is given as a specific example, and other orientations (e.g., spinning in  $yz$  and sensing along  $x$ ) are possible and have been implemented here.

(44), has electrodes separated by 4 mm and an aperture size of 2 mm. Any configuration of voltages can be applied to the electrodes, producing specific electric field configurations at the location of the MS. The long-term stability of the three-dimensional location is measured by an auxiliary imaging system, which is used to compensate for slow drifts in  $z$  of the MS, maintaining the initial position with submicrometer precision throughout the entire calibration procedure and measurement period.

### Modeling electrostatic forces on a trapped MS

Consider a trapped MS with a monopole charge  $q$ , and permanent dipole moment with magnitude  $p_0$ , subjected to an applied electric field  $\mathbf{E}_{ac}$  oscillating at  $f_0$  along the  $z$  axis (for rotation in  $xy$ ), as well as a stray DC field  $\mathbf{E}_{dc}$  that is assumed to be constant in time.

The application of an additional rotating field,  $\mathbf{E}_{spin}$ , spins the sphere in the  $xy$  plane (Fig. 1), and given that the rotation frequency is much higher than  $f_0$ , the effective dipole moment is averaged out, with a possible remaining effective value,  $\mathbf{p}_{dc}$ , due to higher-order electric moments or imperfect alignment between the electric fields and the optical axes of the trap. The resulting force on the MS at  $f_0$  can be separated into three distinct terms for individual consideration

$$\mathbf{F} = \underbrace{q\mathbf{E}_{ac}}_{\text{Monopole}} + \underbrace{\mathbf{p}_{dc} \cdot \nabla \mathbf{E}_{ac}}_{\text{Permanent dipole}} + \underbrace{\mathbf{p}_{ac} \cdot \nabla \mathbf{E}_{dc}}_{\text{Induced dipole}} \quad (1)$$

with  $\mathbf{p}_{dc}$  being the time-averaged projection of the residual permanent dipole moment and  $\mathbf{p}_{ac}$  being the oscillating dipole moment induced by the applied electric field.

When biasing individual electrodes, the ‘‘Monopole’’ term in Eq. 1 is expected to have the opposite sign for opposing electrodes because  $\mathbf{E}_{ac}$  is always oriented toward (away from) the electrode producing the field when the applied voltage is positive (negative).

The ‘‘Permanent dipole’’ term represents the interaction of the permanent dipole moment of the MS with electrical field gradients. This interaction has been the principal limitation for using levitated MS to search for new physics involving monopole charges (24, 25).

Unlike the monopole response, the contribution from the permanent dipole moment with a fixed orientation has the same sign for an electric field from each of two opposing electrodes. Hence, a new differential measurement scheme in which the permanent dipole contribution is dynamically canceled can be introduced. Let  $\mathbf{F}^+$  ( $\mathbf{F}^-$ ) be the force on the trapped MS due to an excitation field  $\mathbf{E}_{ac}$  sourced by the  $z^+$  ( $z^-$ ) electrodes, respectively, defined explicitly in the Supplementary Materials. Let  $F^\pm$  be the projections of  $\mathbf{F}^\pm$  along the  $z$  axis where the sensing field is applied, so that the permanent dipole contribution to  $F^\pm$  can be eliminated by constructing a combined response parameter  $A$

$$A \equiv F^+ - \eta F^- = 2qE^+ + (p_{ac}^+ - \eta p_{ac}^-) \frac{\partial E_{dc,z}}{\partial z} \quad (2)$$

with  $\eta \equiv |\partial_z E^+| / |\partial_z E^-| = |E^+| / |E^-|$ , a constant set by the alignment of the optical trap to the center of the electrode cube. The key point of this construction is the fact that  $\text{sgn}(E^+) = -\text{sgn}(E^-)$  as naively expected, but  $\text{sgn}(\partial_z E^+) = \text{sgn}(\partial_z E^-)$ , which yields to the cancellation of the permanent dipole contribution. The value for  $\eta$  used in our analysis is extracted from a finite element analysis (FEA) of field gradients for the electrode geometry at the measured position of the MS. The position is measured with a submicrometer resolution as explained below. The drift in the position throughout each measurement is at submicrometer level as well, which, in turn, translates into stability in  $\eta$  at the subpercent level. Therefore, the cancellation of the permanent dipole moment is expected to work down to the subpercent level as well.

During a measurement sequence, the excitation sinusoidal field is sourced first from the  $z^+$  electrode for 10 s. This is followed by a  $\mathcal{O}(1\text{-s})$  segment, where  $\mathbf{E}_{ac}$  is turned off and  $\mathbf{E}_{spin}$  remains on, realigning the MS dipole moment to rotate within the  $xy$  plane, correcting for any excursions that  $\mathbf{E}_{ac}$  may have introduced. Afterward, the oscillating voltage is applied to the opposing electrode,  $z^-$ , for another 10 s, completing a single measurement sequence that is repeated for statistical robustness.

The ‘‘Induced dipole’’ term in Eq. 1 is not eliminated by the construction of the combined response parameter  $A$ . However, this

contribution can be evaluated by introducing another construction,  $B$ , for the combined response at the second harmonic

$$B \equiv G^+ - \eta^2 G^- = -\frac{1}{2}(p_{ac}^+ - \eta p_{ac}^-) \frac{\partial E^+}{\partial z} \quad (3)$$

Here,  $G^+$  ( $G^-$ ) is the response amplitude at  $2f_0$ , when the  $z^+$  ( $z^-$ ) electrode is driven. It can be seen that  $B$  is proportional to the remaining induced dipole component in  $A$ . By combining Eqs. 2 and 3, the monopole response can be isolated

$$2qE^+ \simeq A + 2B \frac{(\partial_z E_{dc,z})}{(\partial_z E^+)} \quad (4)$$

where  $E_{dc}$  is the stray electric field in the vicinity of the sphere. Assuming that  $E_{dc}$  is originating from the stray voltages on the electrodes, measured to be on the order of 10 mV, and taking into account the nominal values of  $B$  ( $\sim 5 \times 10^{-16}$  N), it is found that the second term on the right-hand side of Eq. 4 is negligible throughout the current measurement. It has to be emphasized that the construction of the parameters  $A$  and  $B$  is advantageous not only to eliminate and describe the contributions of the dipole moments but also to isolate those contributions and study them to learn about the dielectric properties of individual MSs under the conditions of the measurement.

### Charge sensing

The measured response of a single MS spinning in the  $xy$  plane, and driven at  $f_0$  along  $\hat{z}$  by the  $z^+$  and  $z^-$  electrodes (one at a time), is shown in Fig. 2 (top) (different orientations of electric fields were used for different MSs). The response is extracted by fitting a sine function to a band-pass-filtered output from the MS's imaging system, where the phase for the fit is extracted from the digitized electrode voltage drive. For the same dataset, the behavior of the combined response parameter  $A$  for the given responses  $F^+$  and  $F^-$  can be seen in Fig. 2 (bottom). The cancellation of the residual permanent dipole effect is evident, and  $A$  is purely limited by the noise floor.

In addition, correlations between  $F^+$  and  $F^-$  in a dataset collected over 90 hours are illustrated in Fig. 3, where the superposed purple and blue lines indicate expected signals due to the MS carrying a

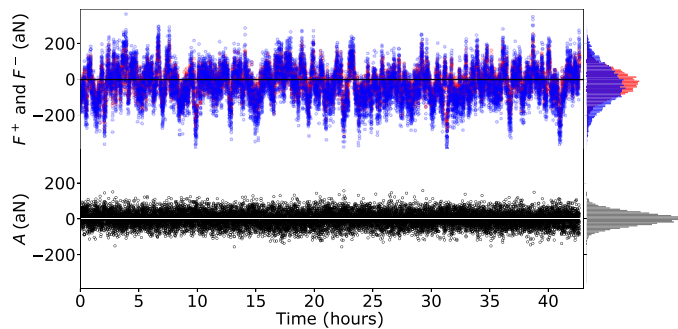


**Fig. 2. MS response over time.** Top: In-phase responses,  $F^+$  and  $F^-$ , of the MS to an oscillating electric field,  $E_{ac}$ , applied sequentially to the  $z^+$  electrode (blue) and the  $z^-$  electrode (red). Each point represents an average value of the response over a 10-s data segment. The drifts in  $F^+$  and  $F^-$  are dominated by slow drifts in the permanent dipole moment. Bottom: Combined response parameter  $A$  for the same data segments as in the top panel. Both panels also show equally binned histograms projected on the response axis.

monopole charge and permanent dipole, respectively. One can see that most of the measured variation is consistent with a permanent dipole moment. This contribution is disentangled and eliminated by the combined response parameter  $A$ . The deviations from the origin along the major axis of the ellipse correspond to excursions of the rotating electric dipole moment from the  $xy$  plane, as well as possible higher-order electric moments.  $|\langle p_{dc} \rangle|$ , the time-averaged value of the residual dipole moment along  $z$ , can be estimated by using  $F^+ + |E^+/E^-| F^- \simeq 2p_{dc} \cdot \nabla E^+$ . For the dataset presented in Figs. 2 and 3, this is consistent with a  $|\langle p_{dc} \rangle| \lesssim 20 e \mu\text{m}$ . The exact value of this contribution in individual 10-s data segments varies with a time scale of few hours. The value is, nevertheless, an order of magnitude smaller than the typical electric dipole moment of a nonspinning MS.

In a similar fashion,  $G^+$  and  $G^-$  can be used to estimate  $p_{ac}^+$  and  $p_{ac}^-$  to be 214 and 318  $e \mu\text{m}$ , respectively. The dominant sources of  $p_{ac}^\pm$  are the inherent polarizability of the MS, expected to be  $\mathcal{O}(10^{-2} e \mu\text{m}/(\text{V/m}))$ , and the oscillations of the dipole moment normal to the plane of rotation driven by  $E_{ac}$ . Those two sources will be investigated in future work, possibly by inducing a change in the polarizability due to faster rotation (47) and/or by applying  $E_{ac}$  in the plane of rotation.

The datasets used for this analysis were taken with three different MSs, at distinct electric field amplitudes, frequencies, spin axes, and overall integration times, as described in Table 1. The charge sensitivity of each MS in the table is estimated by fitting a Gaussian to the distribution of  $A$  (Fig. 2, bottom right). The mean value of each fit is compatible with zero.

To combine the datasets of the three different MSs and to set an upper limit on the monopole charge of the sphere,  $q$ , we follow the likelihood-based procedure outlined in (48). For this purpose, we construct a Gaussian likelihood function on the measured charge

$$\mathcal{L}(q) = \prod_{ij} \frac{1}{\sqrt{2\pi\sigma_{ij}^2}} \exp \left\{ -\frac{[A_{ij}/2E_i^+ - q]^2}{2\sigma_{ij}^2} \right\} \quad (5)$$

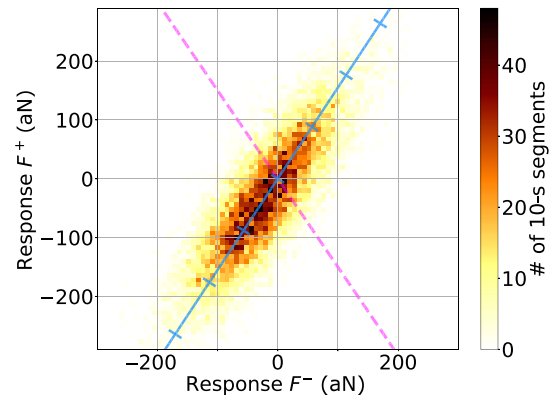


**Fig. 3.  $F^+$  and  $F^-$  correlation.** In-phase force responses,  $F^+$  and  $F^-$ , of an MS, integrated over 10 s. Voltages are applied sequentially to the  $z^+$  and  $z^-$  electrodes, respectively. The data have been binned for illustration as indicated by the color scale. The dashed purple line represents an expected signal from the sphere carrying a monopole charge. The solid blue line represents the response expected from interaction of permanent dipole moments of varying magnitudes, with  $E_{ac}$ . Ticks on the blue line are separated by 25  $e \mu\text{m}$ .

**Table 1. Electric field configuration, where the value of the electric field for analysis is derived from the FEA.** The field strength can be approximated as  $|\mathbf{E}_{xi}| \sim 0.65\Delta V/\Delta x_i$ , with  $\Delta x_i$  being the relevant electrode separation.

| MS | Oscillating field      |                     |      | Electrode separation | Integration time | Charge sensitivity     |
|----|------------------------|---------------------|------|----------------------|------------------|------------------------|
|    | Voltage ( $\Delta V$ ) | Frequency ( $f_0$ ) | Axis |                      |                  |                        |
| 1  | 20 V                   | 71 Hz               | x    | $\Delta x = 8.6$ mm  | 27 hours         | $4.5 \times 10^{-4} e$ |
| 2  | 200 V                  | 71 Hz               | y    | $\Delta y = 8.6$ mm  | 28 hours         | $7.7 \times 10^{-5} e$ |
| 3  | 200 V                  | 139 Hz              | z    | $\Delta z = 4$ mm    | 92 hours         | $3.9 \times 10^{-5} e$ |

Here, the index  $i$  is running over the three MSs, and the index  $j$  is running over all measured  $A$  for a given sphere. The SD,  $\sigma_{ij}$ , is estimated using the same fitting algorithm used to extract  $A$  but on a sideband frequency separated from  $f_0$  by 1 Hz, sufficient to exclude any contribution from the component at  $f_0$ . The combined sensitivity ( $\pm 1\sigma$ ) of the measurement is  $3.3 \times 10^{-5} e$ , and the combined result is compatible with the no-monopole charge hypothesis. This represents the first high-sensitivity, background-free search for monopole interactions using optically levitated MSs. The absence of any monopole signal can be translated into a limit on the abundance of MCP bound to matter that is competitive with the existing state-of-the-art measurements (24, 25) and complementary to other searches for MCPs (49–59). Alternatively, the data can be used to set a limit on the neutrality of matter, although with a lower sensitivity compared to (32–34). Details of these two interpretations are presented in the Supplementary Materials.

## DISCUSSION

The technique illustrated here is only limited by the signal-to-noise ratio (SNR) of the current setup. Figure 4 summarizes possible charge sensitivity improvements as a function of the two parameters responsible for the SNR: the strength of  $\mathbf{E}_{ac}$  and the relative noise sensitivity, normalized to the current setup. The electric field strength is now limited by the existing instruments and can be increased with careful upgrade of the electrode configuration and vacuum feed-throughs. The relative noise sensitivity can be increased by extending the measurement time, assuming the integrability of noise, and by reducing the inherent force noise of the system. The expected Brownian motion of the MS at the vacuum level achieved, is estimated to be  $\sim 10^{-18} \text{ N}/\sqrt{\text{Hz}}$ , which is subdominant at this point and can be reduced further in the future by improving the vacuum. This is also confirmed by the observation that the noise floor is the same at different pressures, below  $10^{-5} \text{ hPa}$ . The shot noise is subdominant as well and estimated to be even lower than the Brownian noise (15, 46). Hence, the observed noise floor is likely technical in nature, dominated by pointing fluctuations of the trapping and reference beams. An enclosure of the input optics, external to the vacuum chamber, is expected to lead to an improvement by a factor of 10 to 100, as demonstrated in (60).

Using parameters that are achievable in the near future, namely, an electric field strength of 150 kV/m, an integration time of  $10^3$  hours, force noise of  $10^{-18} \text{ N}/\sqrt{\text{Hz}}$ , and the background rejection abilities demonstrated in this study, a charge sensitivity of  $\sim 4 \times 10^{-8} e$  is expected. Such a sensitivity would be sufficient to improve

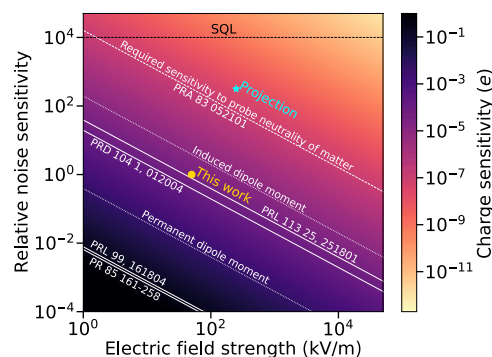


**Fig. 4. Charge sensitivity (color coding) as a function of electric field strength and noise sensitivity relative to the presented result.** Previous experiments (24, 25, 67, 68) have been added as contours of charge sensitivity. In addition, a typical signal arising from a permanent dipole moment of the order of  $\mathcal{O}(100 e \mu\text{m})$  has been added. While the particular magnitude is specific to the gradients in the presented setup, signals of this order have been observed in all techniques sensitive to the dipole moment of a levitated MS (22, 24, 65). On the basis of the presented setup and estimated stray fields sourced by contact potentials of  $\mathcal{O}(10 \text{ mV})$ , an expected signal from the induced dipole at the driving frequency has also been added as a charge sensitivity contour. Once this signal has been properly measured, as the contribution was observed to be negligible in the current work, nothing prohibits further extension of the reach of the technique. A future projection of the presented experiment is added, where an improvement of the relative noise sensitivity by a factor of 300 and an increase of the electric field by a factor of five have been assumed. A measurement with this charge sensitivity could easily improve on the existing limits on the measurement of neutrality of matter (dashed line) for the given MS. A possible future limitation by the standard quantum limit (SQL) is indicated and calculated from the radiation pressure using the same sized MS.

the measurement of the neutrality of matter by about an order of magnitude over the current limit. The sensitivity could be further enhanced by using larger MS, assuming no degradation of noise performance.

Figure 4 also shows the relative noise sensitivity due to the standard quantum limit (SQL) for a  $\mathcal{O}(10\text{-}\mu\text{m})$ -sized sphere. At that level, a charge sensitivity of  $\mathcal{O}(10^{-11} e)$  would be achievable. To bridge the gap between the SQL and the current best realized sensitivity (60), several classical noise sources have to be mitigated, principal among them being gas damping noise that would require reaching pressures of  $\mathcal{O}(10^{-9} \text{ hPa})$ . While a detailed budget of these effects is beyond the scope of this paper, the requirements needed to reach the SQL are well within the reach of existing technology and have already been realized by other levitation techniques (61–64).



We have presented the first background-free search for charges much smaller than the electron charge  $e$ , with an optically levitated macroscopic sensor. By modeling and eliminating contributions due to the permanent dipole moment interacting with electric field gradients, a force noise-limited charge sensitivity of  $3.3 \times 10^{-5} e$  was achieved. Measured data from three different MSs have been analyzed using a profile likelihood method to explore the parameter space for MCPs and the overall neutrality of matter. No monopole signal excess has been found in the present iteration of the experiment. With modest improvements of the setup, a future iteration of the experiment can be competitive with, or improve upon, the current leading experiments probing the neutrality of matter and searching for fifth forces. An exciting future prospect lies in applying this technique to perform metrology on the electromagnetic properties of levitated objects, such as their polarizability and permittivity, in situ. This will enable a more detailed understanding of the dynamics of such objects, necessary to push the boundaries of the technology toward the quantum limit.

## MATERIALS AND METHODS

### Force calibration and MS dipole stabilization

MSs usually carry a net charge when initially trapped, but their charge state can be altered in units of electron charge, by removing or adding individual electrons using ultraviolet photons from a xenon flash lamp. A  $\mathcal{O}(100\text{-Hz})$  sinusoidal electric field with  $\mathcal{O}(100\text{-V})$  amplitude is applied with pairs of opposing electrodes, for the purpose of measuring the charge state and calibrating the MS response to applied forces. This can be achieved when the charge imbalance is of only a few  $\pm 1 e$ , as the charge quantization becomes apparent with an exceedingly large SNR (24, 46). The MS is subsequently discharged to apparent net neutrality.

During this calibration procedure, the response of the MS to a sinusoidal electric field applied to a single electrode, with all others grounded, is also measured. From this, the position of the MS (set by the trapping laser) relative to the centers of the three pairs of electrodes can be estimated with a submicrometer resolution (65). This is done by comparing the ratio of the response to two opposing electrodes to the expected electric field ratio calculated with FEA. This is distinct from the nominal force calibration performed earlier, wherein opposing electrodes are driven simultaneously to minimize gradients at the trap location.

Next, a rotating electrical field ( $\mathbf{E}_{\text{spin}}$ ) is applied (indicated by oscillating voltages applied to the  $x^{\pm}$  and  $y^{\pm}$  electrodes in Fig. 1). This electric field applies a torque to the electric dipole moment that trapped MSs generally appear to carry (7, 14, 65, 66), inducing the MS to rotate in the  $xy$  plane with an angular velocity set by the frequency of the rotating field. Typical electric fields have a frequency of  $\sim 100$  kHz and an amplitude of  $\sim 50$  kV/m. The plane of rotation can be set arbitrarily, and here, rotation in the  $xy$  plane is used as a concrete example.

## SUPPLEMENTARY MATERIALS

Supplementary material for this article is available at <https://science.org/doi/10.1126/sciadv.abo2361>

## REFERENCES AND NOTES

- C. Gonzalez-Ballester, M. Aspelmeyer, L. Novotny, R. Quidant, O. Romero-Isart, Levitodynamics: Levitation and control of microscopic objects in vacuum. *Science* **374**, eabg3027 (2021).
- L. Magrini, P. Rosenzweig, C. Bach, A. Deutschmann-Olek, S. G. Hofer, S. Hong, N. Kiesel, A. Kugi, M. Aspelmeyer, Real-time optimal quantum control of mechanical motion at room temperature. *Nature* **595**, 373–377 (2021).
- F. Tebbenjohanns, M. L. Mattana, M. Rossi, M. Frimmer, L. Novotny, Quantum control of a nanoparticle optically levitated in cryogenic free space. *Nature* **595**, 378–382 (2021).
- J. Gieseler, B. Deutsch, R. Quidant, L. Novotny, Subkelvin parametric feedback cooling of a laser-trapped nanoparticle. *Phys. Rev. Lett.* **109**, 103603 (2012).
- V. Jain, J. Gieseler, C. Moritz, C. Dellago, R. Quidant, L. Novotny, Direct measurement of photon recoil from a levitated nanoparticle. *Phys. Rev. Lett.* **116**, 243601 (2016).
- F. Monteiro, S. Ghosh, E. C. van Assendelft, D. C. Moore, Optical rotation of levitated spheres in high vacuum. *Phys. Rev. A* **97**, 051802 (2018).
- A. D. Rider, C. P. Blakemore, A. Kawasaki, N. Priel, S. Roy, G. Gratta, Electrically driven, optically levitated microscopic rotors. *Phys. Rev. A* **99**, 041802 (2019).
- R. Reimann, M. Doderer, E. Hebestreit, R. Diehl, M. Frimmer, D. Windey, F. Tebbenjohanns, L. Novotny, Ghz rotation of an optically trapped nanoparticle in vacuum. *Phys. Rev. Lett.* **121**, 033602 (2018).
- T. M. Hoang, Y. Ma, J. Ahn, J. Bang, F. Robicheaux, Z.-Q. Yin, T. Li, Torsional optomechanics of a levitated nonspherical nanoparticle. *Phys. Rev. Lett.* **117**, 123604 (2016).
- T. Delord, P. Huillery, L. Nicolas, G. Hétet, Spin-cooling of the motion of a trapped diamond. *Nature* **580**, 56–59 (2020).
- J. Ahn, Z. Xu, J. Bang, Y.-H. Deng, T. M. Hoang, Q. Han, R.-M. Ma, T. Li, Optically levitated nanodumbbell torsion balance and GHz nanomechanical rotor. *Phys. Rev. Lett.* **121**, 033603 (2018).
- B. A. Stickler, K. Hornberger, M. S. Kim, Quantum rotations of nanoparticles. *Nat. Rev. Phys.* **3**, 589–597 (2021).
- A. A. Geraci, S. B. Papp, J. Kitching, Short-range force detection using optically-cooled levitated microspheres. *Phys. Rev. Lett.* **105**, 101101 (2010).
- A. D. Rider, D. C. Moore, C. P. Blakemore, M. Louis, M. Lu, G. Gratta, Search for screened interactions associated with dark energy below the 100  $\mu\text{m}$  length scale. *Phys. Rev. Lett.* **117**, 101101 (2016).
- C. P. Blakemore, A. Fieguth, A. Kawasaki, N. Priel, D. Martin, A. D. Rider, Q. Wang, G. Gratta, Search for non-Newtonian interactions at micrometer scale with a levitated test mass. *Phys. Rev. A* **104**, L061101 (2021).
- P. Fadeev, Y. V. Stadnik, F. Ficek, M. G. Kozlov, V. V. Flambaum, D. Budker, Revisiting spin-dependent forces mediated by new bosons: Potentials in the coordinate-space representation for macroscopic- and atomic-scale experiments. *Phys. Rev. A* **99**, 022113 (2019).
- D. C. Moore, A. A. Geraci, Searching for new physics using optically levitated sensors. *Quant. Sci. Technol.* **6**, 014008 (2021).
- A. Arvanitaki, A. A. Geraci, Detecting high-frequency gravitational waves with optically levitated sensors. *Phys. Rev. Lett.* **110**, 071105 (2013).
- N. Aggarwal, G. P. Winstone, M. Teo, M. Baryakhtar, S. L. Larson, V. Kalogera, A. A. Geraci, Searching for new physics with a levitated-sensor-based gravitational-wave detector. *Phys. Rev. Lett.* **128**, 111101 (2020).
- D. Carney, G. Krnjaic, D. C. Moore, C. A. Regal, G. Afek, S. Bhave, B. Brubaker, T. Corbitt, J. Cripe, N. Crisosto, A. Geraci, S. Ghosh, J. G. E. Harris, A. Hook, E. W. Kolb, J. Kunjummen, R. F. Lang, T. Li, Z. Liu, Z. Liu, J. Lykken, L. Magrini, J. Manley, N. Matsumoto, A. Monte, F. Monteiro, T. Purdy, C. J. Riedel, R. Singh, S. Singh, K. Sinha, J. M. Taylor, J. Qin, D. J. Wilson, Y. Zhao, Mechanical quantum sensing in the search for dark matter. *Quant. Sci. Technol.* **6**, 024002 (2021).
- F. Monteiro, G. Afek, D. Carney, G. Krnjaic, J. Wang, D. C. Moore, Search for composite dark matter with optically levitated sensors. *Phys. Rev. Lett.* **125**, 181102 (2020).
- G. Afek, D. Carney, D. C. Moore, Coherent scattering of low mass dark matter from optically trapped sensors. *Phys. Rev. Lett.* **128**, 101301 (2022).
- A. Kawasaki, Search for kilogram-scale dark matter with precision displacement sensors. *Phys. Rev. A* **99**, 023005 (2019).
- D. C. Moore, A. D. Rider, G. Gratta, Search for millicharged particles using optically levitated microspheres. *Phys. Rev. Lett.* **113**, 251801 (2014).
- G. Afek, F. Monteiro, J. Wang, B. Siegel, S. Ghosh, D. C. Moore, Limits on the abundance of millicharged particles bound to matter. *Phys. Rev. D* **104**, 012004 (2021).
- C. P. Blakemore, A. D. Rider, S. Roy, Q. Wang, A. Kawasaki, G. Gratta, Three-dimensional force-field microscopy with optically levitated microspheres. *Phys. Rev. A* **99**, 023816 (2019).
- C. W. F. Everitt, D. B. DeBra, B. W. Parkinson, J. P. Turneaure, J. W. Conklin, M. I. Heifetz, G. M. Keiser, A. S. Silbergleit, T. Holmes, J. Kolodziejczak, M. al-Meshari, J. C. Mester, B. Muhlfelder, V. G. Solomonik, K. Stahl, P. W. Worden, W. Benze, S. Buchman, B. Clarke, A. al-Jadaani, H. al-Jibreen, J. Li, J. A. Lipa, J. M. Lockhart, B. al-Suwaidan, M. Taber, S. Wang, Gravity probe B: Final results of a space experiment to test general relativity. *Phys. Rev. Lett.* **106**, 221101 (2011).
- S. Buchman, J. P. Turneaure, The effects of patch-potentials on the gravity probe B gyroscopes. *Rev. Sci. Instrum.* **82**, 074502 (2011).

29. M. Armano, H. Audley, G. Auger, J. T. Baird, P. Binetruy, M. Born, D. Bortoluzzi, N. Brandt, A. Bursi, M. Caleno, A. Cavalleri, A. Cesarini, M. Cruise, K. Danzmann, M. de Deus Silva, I. Diepholz, R. Dolesi, N. Dunbar, L. Ferraioli, V. Ferroni, E. D. Fitzsimons, R. Flatscher, M. Freschi, J. Gallegos, C. Garcia-Marin, R. Gerndt, L. Gesa, F. Gibert, D. Giardini, R. Giusteri, C. Grimani, J. Grzymisch, I. Harrison, G. Heinzl, M. Hewitson, D. Hollington, M. Hueller, J. Huesler, H. Inchauspé, O. Jennrich, P. Jetzer, B. Johlander, N. Karnesis, B. Kaune, C. J. Killow, N. Korsakova, I. Lloro, L. Liu, J. P. López-Zaragoza, R. Maarschalkerweerd, S. Madden, D. Mance, V. Martin, L. Martin-Polo, J. Martino, F. Martin-Porqueras, I. Mateos, P. W. McNamara, J. Mendes, L. Mendes, A. Moroni, M. Nofrarias, S. Paczkowski, M. Perreux-Lloyd, A. Petiteau, P. Pivato, E. Plagnol, P. Prat, U. Ragnit, J. Ramos-Castro, J. Reiche, J. A. Romera Perez, D. I. Robertson, H. Rozemeyer, F. Rivas, G. Russano, P. Sarra, A. Schleicher, J. Slutsky, C. Sopuerta, T. J. Sumner, D. Texier, J. I. Thorpe, C. Trenkel, D. Vetrugno, S. Vitale, G. Wanner, H. Ward, P. J. Wass, D. Wealthy, W. J. Weber, A. Wittchen, C. Zanoni, T. Ziegler, P. Zweifel; LISA Pathfinder Collaboration, Charge-induced force noise on free-falling test masses: Results from LISA Pathfinder. *Phys. Rev. Lett.* **118**, 171101 (2017).
30. J. L. Garrett, D. Somers, J. N. Munday, The effect of patch potentials in casimir force measurements determined by heterodyne kelvin probe force microscopy. *J. Phys. Condens. Matter* **27**, 214012 (2015).
31. J. G. Lee, "A Fourier-Bessel test of the gravitational inverse-square law," thesis, University of Washington (2020).
32. G. Bressi, G. Carugno, F. Della Valle, G. Galeazzi, G. Ruoso, G. Sartori, Testing the neutrality of matter by acoustic means in a spherical resonator. *Phys. Rev. A* **83**, 052101 (2011).
33. G. Gallinaro, M. Marinelli, G. Morpurgo, Electric neutrality of matter. *Phys. Rev. Lett.* **38**, 1255–1258 (1977).
34. H. F. Dylla, J. G. King, Neutrality of molecules by a new method. *Phys. Rev. A* **7**, 1224–1229 (1973).
35. M. I. Dobroliubov, A. Y. Ignatiev, Millicharged particles. *Phys. Rev. Lett.* **65**, 679–682 (1990).
36. J. Jaeckel, A. Ringwald, The low-energy frontier of particle physics. *Annu. Rev. Nuclear Particle Sci.* **60**, 405–437 (2010).
37. O. Klein, The atomicity of electricity as a quantum theory law. *Nature* **118**, 516 (1926).
38. P. A. M. Dirac, Quantised singularities in the electromagnetic field. *Proc. R. Soc. A* **133**, 60–72 (1931).
39. M. Pospelov, A. Ritz, M. B. Voloshin, Secluded wimp dark matter. *Phys. Lett. B* **662**, 53–61 (2008).
40. C. Boehm, P. Fayet, Scalar dark matter candidates. *Nuclear Phys. B* **683**, 219–263 (2004).
41. S. D. McDermott, H.-B. Yu, K. M. Zurek, Turning off the lights: How dark is dark matter? *Phys. Rev. D* **83**, 063509 (2011).
42. D. Budker, P. W. Graham, H. Ramani, F. Schmidt-Kaler, C. Smorra, S. Ulmer, Millicharged dark matter detection with ion traps. *PRX Quant.* **3**, 010330 (2022).
43. microParticles Onlineshop (microParticles GmbH), <https://www.microparticles-shop.de/>.
44. C. P. Blakemore, "Fundamental and applied physics with optically levitated microspheres," thesis, Stanford University (2021).
45. A. Ashkin, J. M. Dziedzic, Optical levitation by radiation pressure. *Appl. Phys. Lett.* **19**, 283–285 (1971).
46. A. Kawasaki, A. Fieguth, N. Priel, C. P. Blakemore, D. Martin, G. Gratta, High sensitivity, levitated microscope apparatus for short-distance force measurements. *Rev. Sci. Instrum.* **91**, 083201 (2020).
47. D. Hümmer, R. Lampert, K. Kustura, P. Maurer, C. Gonzalez-Ballester, O. Romero-Isart, Acoustic and optical properties of a fast-spinning dielectric nanoparticle. *Phys. Rev. B* **101**, 205416 (2020).
48. G. Cowan, K. Cranmer, E. Gross, O. Vitells, Asymptotic formulae for likelihood-based tests of new physics. *Eur. Phys. J. C* **71**, 1554 (2011).
49. A. A. Prinz, R. Baggs, J. Ballam, S. Ecklund, C. Fertig, J. A. Jaros, K. Kase, A. Kulikov, W. G. J. Langeveld, R. Leonard, T. Marvin, T. Nakashima, W. R. Nelson, A. Odian, M. Pertsova, G. Putallaz, A. Weinstein, Search for millicharged particles at SLAC. *Phys. Rev. Lett.* **81**, 1175–1178 (1998).
50. The CMS collaboration, Searches for long-lived charged particles in pp collisions at  $\sqrt{s} = 7$  and 8 TeV. *J. High Energy Phys.* **07**, 122 (2013).
51. S. Davidson, B. Campbell, D. Bailey, Limits on particles of small electric charge. *Phys. Rev. D* **43**, 2314–2321 (1991).
52. A. Badertscher, P. Crivelli, W. Fetscher, U. Gendotti, S. Gninenko, V. Postoev, A. Rubbia, V. Samoylenko, D. Sillou, An improved limit on invisible decays of positronium. *Phys. Rev. A* **75**, 032004 (2007).
53. S. N. Gninenko, N. V. Krasnikov, A. Rubbia, New limit on millicharged particles from reactor neutrino experiments and the PVLAS anomaly. *Phys. Rev. A* **75**, 075014 (2007).
54. N. Vinyoles, H. Vogel, Minicharged particles from the sun: A cutting-edge bound. *J. Cosmol. Astropart. Phys.* **03**, 002 (2016).
55. S. Davidson, S. Hannestad, G. Raffelt, Updated bounds on millicharged particles. *J. High Energy Phys.* **05**, 003 (2000).
56. M. Mori, Y. Oyama, A. Suzuki, K. Takahashi, M. Yamada, K. Miyano, H. Miyata, H. Takei, K. S. Hirata, T. Kajita, K. Kihara, M. Nakahata, K. Nakamura, S. Ohara, N. Sato, Y. Suzuki, Y. Totsuka, Y. Yaginuma, M. Koshihata, T. Suda, T. Tajima, Y. Fukuda, Y. Nagashima, M. Takita, K. Kaneyuki, T. Tanimori, E. W. Beier, E. D. Frank, W. Frati, S. B. Kim, A. K. Mann, F. M. Newcomer, V. B. Res, W. Zhang, Search for fractionally charged particles in Kamiokande II. *Phys. Rev. A* **43**, 2843–2846 (1991).
57. S. I. Alvisi, I. J. Aronson, F. T. Avignone, A. S. Barabash, C. J. Barton, F. E. Bertrand, V. Brudanin, M. Busch, M. Buuck, T. S. Caldwell, Y. D. Chan, C. D. Christofferson, P. H. Chu, C. Cuesta, J. A. Detwiler, C. Dunagan, Y. Efremenko, H. Ejiri, S. R. Elliott, T. Gilliss, G. K. Giovanetti, M. P. Green, J. Gruszko, I. S. Guinn, V. E. Guiseppe, C. R. Haufe, L. Hehn, R. Henning, E. W. Hoppe, M. A. Howe, S. I. Kononov, R. T. Kouzes, A. M. Lopez, R. D. Martin, R. Massarczyk, S. J. Meijer, S. Mertens, J. Myslik, C. O'Shaughnessy, G. Othman, W. Pettus, A. W. P. Poon, D. C. Radford, J. Rager, A. L. Reine, K. Rielage, R. G. H. Robertson, N. W. Ruof, B. Shanks, M. Shirchenko, A. M. Suriano, D. Tedeschi, R. L. Varner, S. Vasilyev, K. Vorren, B. R. White, J. Y. Wilkerson, C. Wiseman, W. Xu, E. Yakushev, C. H. Yu, V. Yumatov, I. Zhitnikov, B. X. Zhu; Majorana Collaboration, First limit on the direct detection of lightly ionizing particles for electric charge as low as  $e/1000$  with the Majorana Demonstrator. *Phys. Rev. Lett.* **120**, 211804 (2018).
58. I. Alkhatib, D. W. P. Amaral, T. Aramaki, I. J. Aronson, I. Atee Langroudy, E. Azadbakht, S. Banik, D. Barker, C. Bathurst, D. A. Bauer, L. V. S. Bezerra, R. Bhattacharyya, M. A. Bowles, P. L. Brink, R. Bunker, B. Cabrera, R. Calkins, R. A. Cameron, C. Cartaro, D. G. Cerdeño, Y. Y. Chang, M. Chaudhuri, R. Chen, N. Chott, J. Cooley, H. Coombes, J. Corbett, P. Cushman, F. de Brienne, M. L. di Vacri, M. D. Diamond, E. Fascione, E. Figueroa-Feliciano, C. W. Fink, K. Fouts, M. Fritts, G. Gerbier, R. Germond, M. Ghaith, S. R. Golwala, H. R. Harris, B. A. Hines, M. I. Hollister, Z. Hong, E. W. Hoppe, L. Hsu, M. E. Huber, V. Iyer, D. Jardin, A. Jastram, V. K. S. Kashyap, M. H. Kelsey, A. Kubik, N. A. Kurinsky, R. E. Lawrence, A. Li, B. Loer, E. Lopez Asamar, P. Lukens, D. B. MacFarlane, R. Mahapatra, V. Mandic, N. Mast, A. J. Mayer, H. Meyer zu Theenhausen, É. M. Michaud, E. Michielin, N. Mirabolfathi, B. Mohanty, J. D. Morales-Mendoza, S. Nagorny, J. Nelson, H. Neog, V. Novati, J. L. Orrell, S. M. Oser, W. A. Page, R. Partridge, R. Podvianiuk, F. Ponce, S. Poudel, A. Pradeep, M. Pyle, W. Rau, E. Reid, R. Ren, T. Reynolds, A. Roberts, A. E. Robinson, T. Saab, B. Sadoulet, J. Sander, A. Sattari, R. W. Schnee, S. Scorza, B. Serfass, D. J. Sincavage, C. Stanford, J. Street, D. Toback, R. Underwood, S. Verma, A. N. Villano, B. von Krosigk, S. L. Watkins, J. S. Wilson, M. J. Wilson, J. Winchell, D. H. Wright, S. Yellin, B. A. Young, T. C. Yu, E. Zhang, H. G. Zhang, X. Zhao, L. Zheng; SuperCDMS Collaboration, Constraints on lightly ionizing particles from CDMSlite. *Phys. Rev. Lett.* **127**, 081802 (2021).
59. G. Magill, R. Plestid, M. Pospelov, Y.-D. Tsai, Millicharged particles in neutrino experiments. *Phys. Rev. Lett.* **122**, 071801 (2019).
60. F. Monteiro, W. Li, G. Afek, C.-I. Li, M. Mossman, D. C. Moore, Force and acceleration sensing with optically levitated nanogram masses at microkelvin temperatures. *Phys. Rev. A* **101**, 053835 (2020).
61. V. Blims, M. Piotrowski, M. I. Hussain, B. G. Norton, S. C. Connell, S. Gensemer, M. Lobino, E. W. Streed, A single-atom 3D sub-attoneutron force sensor. *Sci. Adv.* **4**, eaa04453 (2018).
62. K. A. Gilmore, J. G. Bohnet, B. C. Sawyer, J. W. Britton, J. J. Bollinger, Amplitude sensing below the zero-point fluctuations with a two-dimensional trapped-ion mechanical oscillator. *Phys. Rev. Lett.* **118**, 263602 (2017).
63. H. Loh, K. C. Cossel, M. C. Grau, K.-K. Ni, E. R. Meyer, J. L. Bohn, J. Ye, E. A. Cornell, Precision spectroscopy of polarized molecules in an ion trap. *Science* **342**, 1220–1222 (2013).
64. A. Vinante, P. Falferi, G. Gasbarri, A. Setter, C. Timberlake, H. Ulbricht, Ultralow mechanical damping with Meissner-levitated ferromagnetic microparticles. *Phys. Rev. Appl.* **13**, 064027 (2020).
65. G. Afek, F. Monteiro, B. Siegel, J. Wang, S. Dickson, J. Recoaro, M. Watts, D. C. Moore, Control and measurement of electric dipole moments in levitated optomechanics. *Phys. Rev. A* **104**, 053512 (2021).
66. C. P. Blakemore, D. Martin, A. Fieguth, A. Kawasaki, N. Priel, A. D. Rider, G. Gratta, Absolute pressure and gas species identification with an optically levitated rotor. *J. Vacuum Sci. Technol. B* **38**, 024201 (2020).
67. P. C. Kim, E. R. Lee, I. T. Lee, M. L. Perl, V. Halyo, D. Loomba, Search for fractional-charge particles in meteoritic material. *Phys. Rev. Lett.* **99**, 161804 (2007).
68. M. Marinelli, G. Morpurgo, Searches of fractionally charged particles in matter with the magnetic levitation technique. *Phys. Rep.* **85**, 161–258 (1982).

**Acknowledgments:** We acknowledge regular discussions on the physics of trapped microspheres with the group of D. Moore at Yale and thank B. Lenardo for providing constructive feedback on the manuscript. **Funding:** This work was supported by the National Science Foundation under grant no. PHY2108244, the Office of Naval Research under grant no. N00014-18-1-2409, and the Heising-Simons Foundation. N.P. is supported, in part, by a grant of the Koret Foundation. C.P.B. acknowledges the partial support of a Gerald J. Lieberman Fellowship of Stanford University. A.K. was partial supported by a William M.

and Jane D. Fairbank Postdoctoral Fellowship of Stanford University. **Author contributions:** N.P. and A.F. developed the measuring technique presented in the paper. N.P., A.F., G.V., and D.M. were involved in data taking. N.P. developed the model. N.P, A.F., and C.P.B. analyzed the data. All authors were involved in building the two systems used in the paper and contributed to the development of the measuring techniques used in the paper. All authors discussed the results and assisted in the manuscript preparation. **Competing interests:** The authors declare that they have no competing interests. **Data and materials availability:**

All data needed to evaluate the conclusions in the paper are present in the paper and/or the Supplementary Materials.

Submitted 21 January 2022

Accepted 22 August 2022

Published 14 October 2022

10.1126/sciadv.abo2361